# Achievable Fixed Rate Capacity in Emerging Wireless Systems

(*Invited Paper)*

Paschalis C. Sofotasios*,‡, Seong Ki Yoo§, Sami Muhaidat*,†, Simon L. Cotton§, F. Javier Lopez-Martinez||, Juan M. Romero-Jerez||, Kahtan Mezher*, and George K. Karagiannidis¶

*Center for Cyber-Physical Systems, Department of Electrical Engineering and Computer Science, Khalifa University, 127788, Abu Dhabi, United Arab Emirates
(e-mail: {paschalis.sofotasios; sami.muhaidat; kahtan.mezher}@ku.ac.ae)
‡Department of Electrical Engineering, Tampere University, FI-33101, Tampere, Finland
(e-mail: paschalis.sofotasios@tuni.fi)
§Institute of Electronics, Communications and Information Technology, Queen's University Belfast, BT3 9DT, Belfast, UK (e-mail: {sk.yoo; simon.cotton}@qub.ac.uk)
†Institute for Communication Systems, University of Surrey, GU2 7XH, Guildford, UK
||Departmento de Ingenieria de Comunicaciones, Universidad de Malaga - Campus de Excelencia Internacional Andalucia Tech., 29071, Malaga, Spain (e-mail: fjlopezm@ic.uma.es; romero@dte.uma.es)
¶Department of Electrical and Computer Engineering, Aristotle University of Thessaloniki, GR-51124, Thessaloniki, Greece (e-mail: geokarag@auth.gr)

***Abstract*—The $\mathcal{F}$ composite fading model was recently proposed as an accurate and tractable statistical model for the characterization of the simultaneous occurrence of multipath fading and shadowing conditions encountered in realistic wireless communication scenarios. In the present contribution we capitalize on the distinct properties of this composite model to derive the achievable capacity over $\mathcal{F}$ composite fading channels assuming fixed rate quality of service requirements. To this end, novel exact and tractable analytic expressions are derived for both the exact and the truncated channel inversion strategies. This also enables the derivation of additional simplified approximate and asymptotic expressions for these cases, which provide meaningful insights on the effect of fading conditions on the overall system performance. This is particularly useful in the context of numerous emerging wireless applications of interest that exhibit stringent fixed rate requirements such as vehicular communications, body area networks and telemedicine, among others.**

## I. Introduction

It is well-known that wireless transmission is subject to multipath fading which is mainly caused by the constructive and destructive interference between two or more versions of the transmitted signal. Since multipath fading is typically detrimental to the performance of wireless communications systems, it is important to characterize and model multipath fading channels accurately in order to understand and improve their behavior and corresponding implications. In this context, numerous fading models such as Rayleigh, Rice and Nakagami-$m$ have been utilized in an attempt to characterize multipath fading, depending on the nature of the radio propagation environment [1]–[4].

Based on the above, extensive analyses on the performance of various wireless communication systems have been reported in [5]–[14] and the references therein. Specifically, the authors in [5]–[7] introduced the concepts of capacity analysis under different adaptation policies and carried out an extensive analysis over Rayleigh and Nakagami-$m$ fading channels. Likewise, the ergodic capacity over correlated Rician fading channels and under generalized fading conditions was investigated in [8] and [9], respectively. In the same context, comprehensive capacity analyses over independent and correlated generalized fading channels were performed in [10]–[12] for different diversity receiver configurations. Also, a lower bound for the ergodic capacity of distributed multiple input multiple output (MIMO) systems was derived in [13], while the effective throughput over generalized multipath fading in multiple input single output (MISO) systems was analyzed in [14].

It is recalled that in most practical wireless scenarios, the transmitted signal may not only undergo multipath fading, but also simultaneous shadowing. The shadowing phenomenon can be typically modeled with the aid of lognormal, gamma, inverse Gaussian and, as shown recently, inverse gamma distributions [15]–[20]. Following from this, the simultaneous occurrence of multipath fading and shadowing can be taken into account using any one of the composite fading models, introduced in the open technical literature [21]–[28]. Capitalizing on this, the performance of digital communications systems over composite fading channels has been analyzed in [29]–[48]. Yet, a corresponding analysis of the channel capacity has been only partially addressed. In addition, most

of the existing studies are either limited to an ergodic capacity analysis for the case of independent and correlated fading channels in conventional, relay and multi-antenna communication scenarios or to the effective capacity and channel capacity under different adaptation policies for the case of conventional communication scenarios. Furthermore, these analyses have been comprehensively addressed only for the case of gamma distributed shadowing and partially for composite models based on lognormal or IG shadowing effects.

Motivated by this, the authors in [49] proposed the use of the Fisher-Snedocor $\mathcal{F}$ distribution to describe the composite fading conditions encountered during realistic wireless transmission. This composite model is based on the key assumption that the root mean square (rms) power of a Nakagami-$m$ signal is subject to variation induced by an inverse Nakagami-$m$ random variable (RV). It was shown in [49] that this assumption renders the $\mathcal{F}$ fading model capable of providing a better fit to measurement data than the widely used generalized-$K$ fading model. Additionally, the algebraic representation of the $\mathcal{F}$ composite fading distribution is fairly tractable and simpler than that of the generalized-$K$ distribution, which until now has been widely regarded as the most analytically tractable composite fading model.

It is recalled that emerging wireless applications are characterized by a high degree of versatility and heterogeneity combined with stringent performance and quality of service requirements. These requirements are largely concerned with significantly high data rates as well as reduced error rates and system outages, and latency. Another, increasingly desired characteristic is the achievement of efficient and robust fixed rate wireless transmission. Fixed rate requirements are highly important in critical conventional and emerging wireless applications relating to vehicular communications as well as in healthcare and telemedicine, where meeting specific quality of service requirements is of paramount importance for health and safety related factors. Therefore, designing effective and robust fixed rate based systems is expected to provide a meaningful solution to several critical wireless applications of interest.

Motivated by the above and given the distinct properties of the recently proposed $\mathcal{F}$ composite fading distribution relating to the combined composite fading modeling accuracy and analytical simplicity, in the present contribution we quantify the achievable fixed rate based channel capacity over $\mathcal{F}$ composite fading channels. To this end, we derive novel exact closed-form expressions for the corresponding channel capacity with channel inversion and fixed rate ($C_{\mathrm{CIFR}}$) and with truncated channel inversion and fixed rate ($C_{\mathrm{TIFR}}$). These expressions have a rather tractable analytic representation which renders them convenient to handle both analytically and numerically. Based on this, they are subsequently used for the derivation of additional simple approximate expressions as well as for expressions in terms of the involved parameters. These representations are meaningful since they provide insights on the effect of the involved parameters on the overall system performance. Hence, they are expected to be useful in the design and deployment of fixed rate systems for critical communication scenarios such as vehicle-to-vehicle communications and telemedicine.

The remainder of the paper is organized as follows: In Section II, we focus on a redefined version of the $\mathcal{F}$ composite fading model. The channel capacity with channel inversion and fixed rate over $\mathcal{F}$ composite fading channels is derived in Section III followed by the channel capacity analysis for truncated channel inversion with fixed rate over $\mathcal{F}$ composite fading channels in Section IV. Corresponding numerical results and useful insights are given in Section V, while concluding remarks are presented in Section VI.

## II. The $\mathcal{F}$ Composite Fading Model

Similar to the physical signal model proposed for the Nakagami-$m$ fading channel [50], the received signal in an $\mathcal{F}$ composite fading channel is composed of separable clusters of multipath in which the scattered waves have similar delay times, with the delay spreads of different clusters being relatively large. However, in contrast to the Nakagami-$m$ signal, in an $\mathcal{F}$ composite fading channel, the rms power of the received signal is subject to random variation induced by shadowing. Based on this, the received signal envelope, $R$, can be expressed as

$$R = \sqrt{\sum_{i=1}^{m} \alpha^2 I_i^2 + \alpha^2 Q_i^2}, \tag{1}$$

where $m$ represents the number of clusters of multipath, $I_i$ and $Q_i$ are independent Gaussian RVs which denote the in-phase and quadrature phase components of the multipath cluster $i$, respectively, where

$$\mathbb{E}[I_i] = \mathbb{E}[Q_i] = 0 \tag{2}$$

and

$$\mathbb{E}[I_i^2] = \mathbb{E}[Q_i^2] = \sigma^2, \tag{3}$$

with $\mathbb{E}[\cdot]$ denoting statistical expectation. In (1), $\alpha$ is a normalized inverse Nakagami-$m$ RV where $m_s$ is the shape parameter and $\mathbb{E}[\alpha^2] = 1$, such that

$$f_\alpha(\alpha) = \frac{2(m_s-1)^{m_s}}{\Gamma(m_s)\ \alpha^{2m_s+1}} \exp\left(-\frac{m_s-1}{\alpha^2}\right), \tag{4}$$

where $\Gamma(\cdot)$ represents the gamma function [51, eq. (8.310.1)].

Following the approach in [49], we can obtain the corresponding PDF[1] of the received signal envelope, $R$, in an $\mathcal{F}$ composite fading channel, namely

[1]It is worth highlighting that in the present paper, we have modified slightly the underlying inverse Nakagami-$m$ PDF from that used in [49] and subsequently the PDF for the $\mathcal{F}$ composite fading model. While the PDF in [49] is completely valid for physical channel characterization, it has some limitations in its admissible parameter range when used in analyses relating to digital communications. The redefined PDF in (5), on the other hand, is well consolidated.

$$f_R(r) = \frac{2\, m^m (m_s-1)^{m_s}\, \Omega^{m_s} r^{2m-1}}{B\left(m, m_s\right)\left[mr^2 + (m_s-1)\,\Omega\right]^{m+m_s}}, \quad (5)$$

which is valid for $m_s > 1$, while $B(\cdot,\cdot)$ denotes the beta function [51, eq. (8.384.1)]. The form of the PDF in (5) is functionally equivalent to the $\mathcal{F}$ distribution[2]. In terms of its physical interpretation, $m$ denotes the fading severity whereas $m_s$ controls the amount of shadowing of the rms signal power. Moreover, $\Omega = \mathbb{E}[r^2]$ represents the mean power. As $m_s \to 0$, the scattered signal component undergoes heavy shadowing; in contrast, as $m_s \to \infty$, there exists no shadowing in the wireless channel and therefore it corresponds to a standard Nakagami-$m$ fading channel. Furthermore, as $m \to \infty$ and $m_s \to \infty$, the $\mathcal{F}$ composite fading model becomes increasingly deterministic, i.e., it becomes equivalent to an additive white Gaussian noise (AWGN) channel.

Based on (5), the PDF of the instantaneous SNR, $\gamma$, in an $\mathcal{F}$ composite fading channel can be straightforwardly deduced using the variable transformation $\gamma = \overline{\gamma} r^2/\Omega$, such that

$$f_\gamma(\gamma) = \frac{m^m (m_s-1)^{m_s}\, \overline{\gamma}^{m_s} \gamma^{m-1}}{B\left(m, m_s\right)\left[m\gamma + (m_s-1)\,\overline{\gamma}\right]^{m+m_s}}, \quad (6)$$

where $\overline{\gamma} = \mathbb{E}[\gamma]$ denotes the corresponding average SNR. To this effect, the redefined moments,

$$\mathbb{E}[\gamma^n] \triangleq \int_0^\infty \gamma^n f_\gamma(\gamma) \mathrm{d}\gamma \quad (7)$$

are expressed as [52]

$$\mathbb{E}[\gamma^n] = \frac{(m_s-1)^n \overline{\gamma}^n \Gamma(m+n)\Gamma(m_s-n)}{m^n \Gamma(m)\Gamma(m_s)}. \quad (8)$$

Similarly, with the aid of [51, eq. (3.194.1)] the envelope cumulative distribution function (CDF) is expressed as

$$\begin{aligned} F_R(r) =& \frac{m^{m-1} r^{2m}}{B(m,m_s)(m_s-1)^m \Omega^m} \\ & \times\, {}_2F_1\left(m, m+m_s, m+1; -\frac{mr^2}{(m_s-1)\Omega}\right), \end{aligned} \quad (9)$$

where ${}_2F_1(\cdot,\cdot;\cdot;\cdot)$ is the Gauss hypergeometric function [51, eq. (9.111)], whereas its respective SNR CDF is readily given by

$$\begin{aligned} F_\gamma(\gamma) =& \frac{m^{m-1} \gamma^m}{B(m,m_s)(m_s-1)^m \overline{\gamma}^m} \\ & \times\, {}_2F_1\left(m, m+m_s, m+1; -\frac{m\gamma}{(m_s-1)\overline{\gamma}}\right). \end{aligned} \quad (10)$$

It is noted that the above CDF expressions are valid for arbitrary values of the fading parameters $m$ and $m_s$. However, an additional expression can be derived for the special case of arbitrary values of $m_s$ and integer values of $m$.

**Lemma 1.** *For $\gamma, \overline{\gamma} \in \mathbb{R}^+$, $m \in \mathbb{N}$ and $m_s > 1$, the outage probability under $\mathcal{F}$ composite fading conditions can be expressed as*

$$\begin{aligned} F_\gamma(\gamma) = \sum_{l=0}^{m-1} \binom{m-1}{l} \frac{(-1)^l}{B(m,m_s)} \Bigg\{ & \frac{1}{m_s+l} \\ & - \frac{(m_s-1)^{m_s+l} \overline{\gamma}^{m_s+l}}{(m_s+l)(m\gamma + (m_s-1)\overline{\gamma})^{m_s+l}} \Bigg\}, \end{aligned} \quad (11)$$

*where $\binom{\cdot}{\cdot}$ denotes the binomial coefficient [51, eq. (1.111)].*

*Proof.* It is recalled that the CDF of the $\mathcal{F}$ composite statistical distribution is given by

$$F_\gamma(\gamma) = \int_0^\gamma \frac{m^m (m_s-1)^{m_s}\, \overline{\gamma}^{m_s} x^{m-1}}{B\left(m, m_s\right)\left[mx + (m_s-1)\,\overline{\gamma}\right]^{m+m_s}} \mathrm{d}x. \quad (12)$$

By setting

$$u = mx + (m_s-1)\overline{\gamma} \quad (13)$$

and after some algebraic manipulations, it follows that

$$\begin{aligned} F_\gamma(\gamma) =& \frac{(m_s-1)^{m_s} \overline{\gamma}^{m_s}}{B(m,m_s)} \\ & \times \int_{(m_s-1)\overline{\gamma}}^{m\gamma + (m_s-1)\overline{\gamma}} \frac{(u-(m_s-1)\overline{\gamma})^{m-1}}{u^{m+m_s}} \mathrm{d}u. \end{aligned} \quad (14)$$

By applying the binomial theorem in [51, eq. (1.111)], one obtains

$$\begin{aligned} F_\gamma(\gamma) =& \frac{(m_s-1)^{m_s} \overline{\gamma}^{m_s}}{B(m,m_s)} \sum_{l=0}^{m-1} \binom{m-1}{l} (1-m_s)^l \overline{\gamma}^l \\ & \times \int_{(m_s-1)\overline{\gamma}}^{m\gamma + (m_s-1)\overline{\gamma}} \frac{1}{u^{m_s+l+1}} \mathrm{d}u \end{aligned} \quad (15)$$

which is valid when $m \in \mathbb{N}$. Consequently, the above integral can be evaluated straightforwardly. Based on this and after some algebraic manipulations, the simplified expression for the CDF in (11) is deduced, which completes the proof. □

The derived expression in Lemma 1 is novel and has a relatively simple algebraic representation. Therefore, it is useful in cumbersome analyses relating to digital communications over $\mathcal{F}$ composite fading channels, where (11) proves intractable to lead to the derivation of useful analytic solutions.

## III. Channel Capacity with Fixed Rate

Most communication systems typically assume a known channel state information (CSI) only at the receiver side. However, in several emerging systems, CSI can be also available at the transmitter as this allows greater flexibility and adaptability, resulting in a more efficient and intelligent overall

[2]Letting $r^2 = x$, $m = d_1/2$, $m_s = d_2/2$, $\Omega = d_2/(d_2-2)$ and performing the required transformation yields the $\mathcal{F}$ distribution, $f_X(x)$, with parameters $d_1$ and $d_2$.

system operation. A typical feature in the case of knowing CSI at the transmitter and at the receiver is the ability to benefit from adaptive transmit power. This is the key process of the so called water-filling approach and in fixed rate systems. In the former, higher power and rate levels are allocated in good fading conditions and less power in severe fading conditions. In the latter, the transmitter adapts the power accordingly in order to maintain a fixed rate at the receiver [52]. These concepts are critical in numerous emerging applications that are characterized by stringent quality of service requirements, such as telemedicine and vehicle to vehicle communications [49]. Subsequently, this section is devoted to the capacity analysis over $\mathcal{F}$ composite fading channels for the channel inversion with fixed rate and for truncated channel inversion with fixed rate.

### A. Channel Inversion with Fixed Rate

This policy ensures a fixed data rate at the receiver by means of inverting the channel and adapting the transmit power accordingly. This is particularly useful in numerous applications where a fixed rate is the core requirement. In what follows, we derive the channel capacity with channel inversion and fixed rate in the presence of $\mathcal{F}$ composite fading conditions [5]–[7], [52].

**Theorem 1.** *For $m, \gamma, \overline{\gamma}, B \in \mathbb{R}^+$ and $m_s > 1$, the channel capacity per unit bandwidth with channel inversion and fixed rate under $\mathcal{F}$ composite fading conditions can be expressed as follows:*

$$\frac{C_{\mathrm{CIFR}}}{B} = \log_2\left(1 + \frac{(m-1)(m_s-1)\,\overline{\gamma}}{m\,m_s}\right). \tag{16}$$

*Proof.* The channel capacity with channel inversion and fixed rate is defined as

$$C_{\mathrm{CIFR}} = B\log_2\left(1 + \frac{1}{\int_0^\infty \frac{f_\gamma(\gamma)}{\gamma}\mathrm{d}\gamma}\right). \tag{17}$$

Therefore, for the case of $\mathcal{F}$ composite fading conditions, we substitute (6) into (16), yielding

$$\frac{C_{\mathrm{CIFR}}}{B} = \log_2\left(1 + \frac{B(m,m_s)m^{-m}(m_s-1)^{-m_s}\overline{\gamma}^{-m_s}}{\int_0^\infty \frac{\gamma^{m-1}}{[m\gamma+(m_s-1)\,\overline{\gamma}\,]^{m+m_s}}\mathrm{d}\gamma}\right). \tag{18}$$

The above integral can be obtained in closed-form using [51, eq. (3.194.3)]. To this end, by making the necessary change of variables and substituting in (18) one obtains

$$\frac{C_{\mathrm{CIFR}}}{B} = \log_2\left(1 + \frac{B(m,m_s)\Gamma(m+m_s)(m_s-1)\,\overline{\gamma}}{m\Gamma(m-1)\Gamma(m_s+1)}\right), \tag{19}$$

which with the aid of the properties of the beta and gamma functions along with some algebraic manipulations yields (16), which completes the proof. □

It is evident that (16) has a rather simple algebraic representation. Furthermore, it is particularly insightful since it can be expressed exactly in terms of the average SNR, namely

$$\overline{\gamma} = \frac{m m_s}{(m-1)(m_s-1)}\left(2^{\frac{C_{\mathrm{CIFR}}}{B}} - 1\right) \tag{20}$$

as well as in terms of the fading parameters $m$ and $m_s$, namely

$$m = \frac{(m_s-1)\overline{\gamma}}{(m_s-1)\overline{\gamma} - m_s\left(2^{\frac{C_{\mathrm{CIFR}}}{B}} - 1\right)} \tag{21}$$

and

$$m_s = \frac{(m-1)\overline{\gamma}}{(m-1)\overline{\gamma} - m\left(2^{\frac{C_{\mathrm{CIFR}}}{B}} - 1\right)} \tag{22}$$

respectively. The above expressions can provide meaningful insight on the impact of the involved parameters on the overall system performance. Also, they are useful in determining the required average SNR values for target quality of service and bandwidth requirements under different multipath fading and shadowing conditions.

### B. Truncated Channel Inversion with Fixed Rate

Channel inversion with fixed rate constitutes a low complexity and effective method to achieve fixed rate communications. However, the main drawback of this technique is the large transmit power requirements in case of deep fades, which are often encountered in realistic communication scenarios. Nonetheless, this practical issue can be resolved by inverting the channel above a fixed cut-off level, namely channel truncation. In what follows, we quantify the channel capacity with truncated channel inversion and fixed rate for the case of $\mathcal{F}$ composite fading conditions.

**Theorem 2.** *For $\gamma, \overline{\gamma}, B \in \mathbb{R}^+$, and $m_s > 1$, the channel capacity per unit bandwidth with truncated channel inversion and fixed rate under $\mathcal{F}$ composite fading conditions can be expressed as*

$$\begin{aligned}\frac{C_{\mathrm{TIFR}}}{B} =& \log_2\left(1 + \frac{B(m,m_s)(m_s+1)m^{m_s}\gamma_0^{m_s+1}}{(m_s-1)^{m_s}\overline{\gamma}^{m_s}\mathcal{D}_1}\right)\\ &\times\left(1 - \frac{m^{m-1}\gamma_{\mathrm{th}}^m\mathcal{D}_2}{B(m,m_s)(m_s-1)^m\overline{\gamma}^m}\right)\end{aligned} \tag{23}$$

*when $m \in \mathbb{R}^+$, and*

$$\begin{aligned}\frac{C_{\mathrm{TIFR}}}{B} =& \log_2\left(1 + \frac{B(m,m_s)}{m(m_s-1)^{m_s}\overline{\gamma}^{m_s}\mathcal{D}_3}\right)\\ &\times\left(1 - \sum_{l=0}^{m-1}\binom{m-1}{l}\frac{(-1)^l}{B(m,m_s)}\frac{1-\mathcal{D}_4}{m_s+l}\right)\end{aligned} \tag{24}$$

*when $m \in \mathbb{N}$. The terms $\mathcal{D}_1$ and $\mathcal{D}_2$ in* (23) *are expressed as*

$$\mathcal{D}_1 = {}_2F_1\left(m_s+1, m+m_s; m_s+2; \frac{(1-m_s)\overline{\gamma}}{m\gamma_0}\right) \tag{25}$$

*and*

$$\mathcal{D}_2 = {}_2F_1\left(m, m+m_s; 1+m; \frac{m\gamma_{\rm th}}{(1-m_s)\overline{\gamma}}\right), \tag{26}$$

*whereas the* $\mathcal{D}_3$ *and* $\mathcal{D}_4$ *terms in* (24) *are given by*

$$\mathcal{D}_3 = \sum_{l=0}^{m-2}\binom{m-2}{l}\frac{(-1)^l(m_s+l+1)^{-1}(m_s-1)^l\overline{\gamma}^l}{(m\gamma_0+(m_s-1)\overline{\gamma})^{m_s+l+1}} \tag{27}$$

*and*

$$\mathcal{D}_4 = \frac{(m_s-1)^{m_s+l}\,\overline{\gamma}^{m_s+l}}{(m\gamma_{\rm th}+(m_s-1)\overline{\gamma})^{m_s+l}}. \tag{28}$$

*Proof.* The channel capacity with truncated channel inversion and fixed rate is defined as

$$C_{\rm TIFR} \triangleq B\log_2\left(1+\frac{1}{\int_{\gamma_0}^{\infty}\frac{f_\gamma(\gamma)}{\gamma}{\rm d}\gamma}\right)\int_{\gamma_0}^{\infty} f_\gamma(\gamma){\rm d}\gamma, \tag{29}$$

which with the aid of (6) for the case of $\mathcal{F}$ composite fading channels and recalling that

$$\int_{\gamma_0}^{\infty} f(x){\rm d}x = 1-\int_0^{\gamma_0} f(x){\rm d}x = 1-P_{\rm out} \tag{30}$$

is expressed as

$$\begin{aligned}\frac{C_{\rm TIFR}}{B} =& \log_2\left(1+\frac{B(m,m_s)}{\int_{\gamma_0}^{\infty}\frac{m^m(m_s-1)^{m_s}\,\overline{\gamma}^{m_s}\gamma^{m-2}}{[m\gamma+(m_s-1)\,\overline{\gamma}\,]^{m+m_s}}{\rm d}\gamma}\right)\\ &\times\left(1-\mathcal{D}_5\int_0^{\gamma_0}\frac{\gamma^{m-1}}{[m\gamma+(m_s-1)\,\overline{\gamma}\,]^{m+m_s}}{\rm d}\gamma\right),\end{aligned} \tag{31}$$

where

$$\mathcal{D}_5 = \frac{m^m(m_s-1)^{m_s}\,\overline{\gamma}^{m_s}}{B(m,m_s)}. \tag{32}$$

Now, recalling that

$$P_{\rm out} \triangleq F(\gamma_{\rm th}) \tag{33}$$

and using (10) for the case of $m\in\mathbb{R}^+$ along with substituting in (31), it follows that

$$\begin{aligned}\frac{C_{\rm TIFR}}{B} =& \log_2\left(1+\frac{1}{\mathcal{D}_5\int_{\gamma_0}^{\infty}\frac{\gamma^{m-2}}{[m\gamma+(m_s-1)\,\overline{\gamma}\,]^{m+m_s}}{\rm d}\gamma}\right)\\ &\times\left(1-\frac{m^{m-1}\gamma_{\rm th}^m\mathcal{D}_2}{B(m,m_s)(m_s-1)^m\overline{\gamma}^m}\right).\end{aligned} \tag{34}$$

The integral in (34) can be expressed in closed-form with the aid of [51, eq. (3.194.1)]. This is achieved by performing the necessary variable transformation and after some algebraic manipulations, which yields (23) for the case of $m\in\mathbb{R}^+$.

Likewise, for the case of $m\in\mathbb{N}$, we apply again $P_{\rm out}\triangleq F(\gamma_{\rm th})$ in (11), which upon substitution in (34), it follows that

$$\begin{aligned}\frac{C_{\rm TIFR}}{B} =& \log_2\left(1+\frac{1}{\mathcal{D}_5\int_{\gamma_0}^{\infty}\frac{\gamma^{m-2}}{[m\gamma+(m_s-1)\,\overline{\gamma}\,]^{m+m_s}}{\rm d}\gamma}\right)\\ &\times\left(1-\sum_{l=0}^{m-1}\binom{m-1}{l}\frac{(-1)^l}{B(m,m_s)}\frac{1-\mathcal{D}_4}{m_s+l}\right).\end{aligned} \tag{35}$$

Therefore, by setting

$$u = m\gamma+(m_s-1)\overline{\gamma} \tag{36}$$

in (35), one obtains

$$\begin{aligned}\frac{C_{\rm TIFR}}{B} =& \log_2\left(1+\frac{m^{m-1}}{\mathcal{D}_5\int_{m\gamma_0+(m_s-1)\overline{\gamma}}^{\infty}\frac{(u-(m_s-1)\overline{\gamma})^{m-2}}{u^{m+m_s}}{\rm d}u}\right)\\ &\times\left(1-\sum_{l=0}^{m-1}\binom{m-1}{l}\frac{(-1)^l}{B(m,m_s)}\frac{1-\mathcal{D}_4}{m_s+l}\right).\end{aligned} \tag{37}$$

To this effect, by applying the binomial theorem in [51, eq. (1.111] in the above integral along with some algebraic manipulations yields

$$\begin{aligned}\frac{C_{\rm TIFR}}{B} =& \log_2\left(1+\frac{B(m,m_s)m^{-1}(m_s-1)^{-m_s}\overline{\gamma}^{-m_s}}{\sum_{l=0}^{m-2}\binom{m-2}{l}(-1)^l(m_s-1)^l\overline{\gamma}^{\,l}\mathcal{D}_6}\right)\\ &\times\left(1-\sum_{l=0}^{m-1}\binom{m-1}{l}\frac{(-1)^l}{B(m,m_s)}\frac{1-\mathcal{D}_4}{m_s+l}\right),\end{aligned} \tag{38}$$

where

$$\mathcal{D}_6 = \int_{m\gamma_0+(m_s-1)\overline{\gamma}}^{\infty} u^{-m_s-l-2}{\rm d}u. \tag{39}$$

It is evident that the above elementary integral can be evaluated straightforwardly; hence, equation (24) is deduced, which completes the proof for the case of $m\in\mathbb{N}$. □

**Remark 1.** *It is noted that the integral in* (34) *can be alternatively expressed in closed-form in terms of the incomplete beta function [51]. As a result, the channel capacity with truncated channel inversion and fixed rate over* $\mathcal{F}$ *composite fading channels can be equivalently expressed as*

$$\begin{aligned}\frac{C_{\rm TIFR}}{B} =& \log_2\left(1+\frac{(-1)^{m_s}B(m,m_s)(1-m_s)\overline{\gamma}}{mB\left(\frac{(1-m_s)\overline{\gamma}}{m\gamma_0};1+m_s,1-m-m_s\right)}\right)\\ &\times\left(1-\frac{m^{m-1}\gamma_{\rm th}^m\mathcal{D}_2}{B(m,m_s)(m_s-1)^m\overline{\gamma}^m}\right),\end{aligned} \tag{40}$$

*which holds for* $m\in\mathbb{R}^+$.

The exact analytic expressions in Theorem 5 are tractable both analytically and numerically. However, capitalizing on them leads to the derivation of an even simpler and insightful approximate expression.

**Proposition 1.** *For $\gamma, \overline{\gamma}, \gamma_0, B \in \mathbb{R}^+$, $m \in \mathbb{N}$, $m_s > 1$ and $\overline{\gamma} >> \gamma_{\rm th}$, the channel capacity per unit bandwidth with truncated channel inversion and fixed rate under $\mathcal{F}$ composite fading conditions can be approximated as follows:*

$$\frac{C_{\rm TIFR}}{B} \approx \log_2 \left( 1 + \frac{B(m, m_s)(m_s - 1)\overline{\gamma}}{m \sum_{l=0}^{m-2} \binom{m-2}{l} \frac{(-1)^l}{m_s + l + 1}} \right). \quad (41)$$

*Proof.* By recalling the case of $m \in \mathbb{N}$ in Theorem 5 and assuming large average SNR values, it follows that (24) can be accurately approximated by the simplified representation in (42), at the top of the next page.

To this effect and by assuming that $\overline{\gamma} >> \gamma_{\rm th}$, (42) reduces to

$$\frac{C_{\rm TIFR}}{B} \approx \log_2 \left( 1 + \frac{B(m, m_s) m^{-1} (m_s - 1)^{-m_s} \overline{\gamma}^{-m_s}}{\sum_{l=0}^{m-2} \binom{m-2}{l} \frac{(-1)^l}{(m_s + l + 1)((m_s - 1)\overline{\gamma})^{m_s + 1}}} \right) \quad (43)$$

which after some algebraic manipulations yields (41), which completes the proof. □

**Remark 2.** *It is noted that the proposed approximation is also tight even for some cases with comparable values of $\overline{\gamma}$ and $\overline{\gamma}_{\rm th}$; as a result, the use of* (41) *in practice is not strictly constrained by the condition $\overline{\gamma} >> \gamma_{\rm th}$ in Proposition 6.*

It is also worth noting that (41) is rather insightful as it can be expressed in terms of $\overline{\gamma}$, namely

$$\overline{\gamma} \approx \frac{2^{\frac{C_{\rm TIFR}^{\rm appr.}}{B}} - 1}{B(m, m_s)(m_s - 1)} \sum_{l=0}^{m-2} \binom{m-2}{l} \frac{(-1)^l m}{m_s + l + 1}. \quad (44)$$

As in the previous scenarios, (44) is useful for target quality of service and bandwidth requirements as it quantifies the required average SNR value for different multipath fading and shadowing conditions.

## IV. Numerical Results

In this section, we utilize the analytic results obtained in the previous sections to quantify the achievable channel capacity with channel inversion and fixed rate. This is realized extensively for various communication scenarios under realistic multipath fading and shadowing conditions.

Likewise, Table I depicts the exact results for the considered $C_{\rm CIRA}$ and $C_{\rm TIFR}$ along with other channel capacity measures such as the effective capacity and the capacity with optimum rate adaptation and with optimum power and rate adaptation. This allows direct comparisons between these measures which quantifies the similarities or differences of them in digital transmission over same fading channels. This provides meaningful insights that can determine the corresponding transceiver design according to different scenarios. For example, when the results of the considered channel inversion based measures are comparable to those of the corresponding ergodic capacity, the necessity for CSI knowledge at the transmitter can be alleviated, which in turn can lead to simpler design and therefore to a complexity reduction. On the contrary, when the differences between these measures are non-negligible, CSI knowledge at the transmitter will be considered even at a cost of a complexity increase.

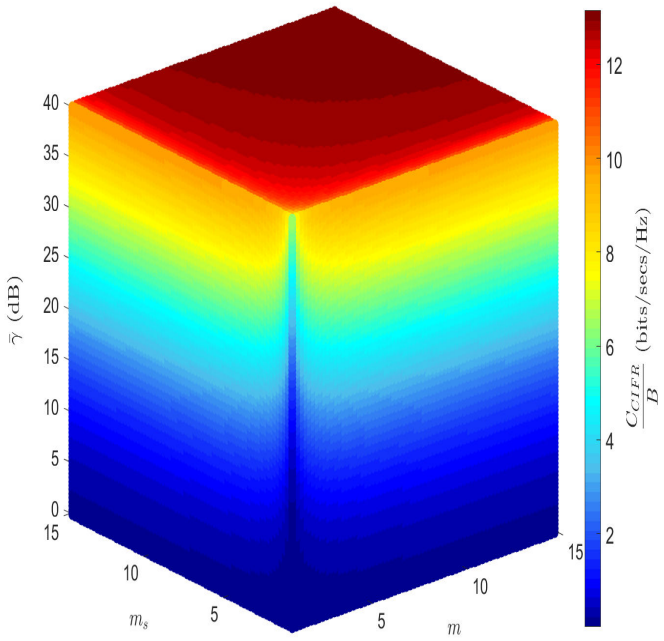


Fig. 1: $C_{\rm CIFR}/{\rm B}$ in an $\mathcal{F}$ fading channel as a function of the $m$, $m_s$ and $\overline{\gamma}$ parameters.

Based on the above, the exact achievable channel capacities are depicted for different fading conditions and average SNR values assuming $A = 2$ for $C_{\rm eff}$ and $\gamma_0 = \gamma_{\rm th} = 2$dB for $C_{\rm OPRA}$ and $C_{\rm TIFR}$. It is shown that the achievable capacities around 0dB are comparable for all types of fading composite fading conditions. However, as the average SNR values increase, we notice larger performance deviations and achievable capacity. Also, the detrimental effect of latency is evident, as this measures exhibits lower performance compared to the other capacity measures. This indicates that latency must be taken into thorough consideration in the determination of the achievable performance limits and hence, in the design and deployment of emerging wireless communication systems with stringent quality of service requirements.

Fig. 1 and Fig. 2 demonstrate the performance of the considered $C_{\rm CIFR}$ and $C_{\rm TIFR}$, respectively, for different values of $m$, $m_s$ and $\overline{\gamma}$ parameters of the $\mathcal{F}$ composite fading channels, namely $1 < m \leq 15$, $1 < m_s \leq 15$ and $0 \leq \overline{\gamma} \leq 40$ dB. It is also noted that the value of $\gamma_0$ for Fig. 2 was set to

$$\frac{C_{\text{TIFR}}^{\text{appr.}}}{B} \approx \log_2\left(1+\frac{B(m,m_s)}{m(m_s-1)^{m_s}\overline{\gamma}^{m_s}\sum_{l=0}^{m-2}\binom{m-2}{l}\frac{(-1)^l(m_s-1)^l\overline{\gamma}^l}{(m_s+l+1)(m\gamma_{\text{th}}+(m_s-1)\overline{\gamma})^{m_s+l+1}}}\right). \quad (42)$$

TABLE I: Exact Channel Capacity with Different Adaptation Policies under $\mathcal{F}$ Fading Conditions.

| Involved Parameters | | | Exact Channel Capacity for $A = 2.0$ and $\gamma_0 = \gamma_{\text{th}} = 2$dB | | | | |
|---|---|---|---|---|---|---|---|
| $m$ | $m_s$ | $\overline{\gamma}$ | $C_{\text{ORA}}$ | $C$eff | $C_{\text{OPRA}}$ | $C_{\text{CIFR}}$ | $C_{\text{TIFR}}$ |
| 1.2 | 1.2 | 0dB | 0.45 | 0.30 | 0.09 | 0.04 | 0.39 |
| 3.2 | 1.2 | 0dB | 0.48 | 0.34 | 0.09 | 0.16 | 0.39 |
| 3.2 | 4.2 | 0dB | 0.90 | 0.75 | 0.10 | 0.61 | 0.63 |
| 6.0 | 6.0 | 0dB | 0.94 | 0.84 | 0.06 | 0.76 | 0.56 |
| 1.2 | 1.2 | 10dB | 1.76 | 1.03 | 0.92 | 0.35 | 1.59 |
| 3.2 | 1.2 | 10dB | 1.92 | 1.27 | 0.98 | 1.10 | 1.67 |
| 3.2 | 4.2 | 10dB | 3.11 | 2.51 | 2.22 | 2.64 | 2.77 |
| 6.0 | 6.0 | 10dB | 3.25 | 2.87 | 2.40 | 2.99 | 3.01 |
| 1.2 | 1.2 | 20dB | 4.27 | 2.39 | 3.48 | 1.92 | 3.32 |
| 3.2 | 1.2 | 20dB | 4.62 | 3.25 | 3.84 | 3.64 | 3.74 |
| 3.2 | 4.2 | 20dB | 6.22 | 5.27 | 5.53 | 5.74 | 5.74 |
| 6.0 | 6.0 | 20dB | 6.40 | 5.89 | 5.72 | 6.14 | 6.14 |
| 1.2 | 1.2 | 30dB | 7.41 | 4.17 | 6.72 | 4.85 | 5.75 |
| 3.2 | 1.2 | 30dB | 7.84 | 6.10 | 7.16 | 6.85 | 6.85 |
| 3.2 | 4.2 | 30dB | 9.52 | 8.47 | 8.85 | 9.04 | 9.04 |
| 6.0 | 6.0 | 30dB | 9.70 | 9.17 | 9.04 | 9.44 | 9.44 |
| 1.2 | 1.2 | 40dB | 10.71 | 6.11 | 10.04 | 8.12 | 8.64 |
| 3.2 | 1.2 | 40dB | 11.15 | 9.31 | 10.48 | 10.16 | 10.16 |
| 3.2 | 4.2 | 40dB | 12.84 | 11.77 | 12.17 | 12.36 | 12.36 |
| 6.0 | 6.0 | 40dB | 13.02 | 12.49 | 12.36 | 12.76 | 12.76 |

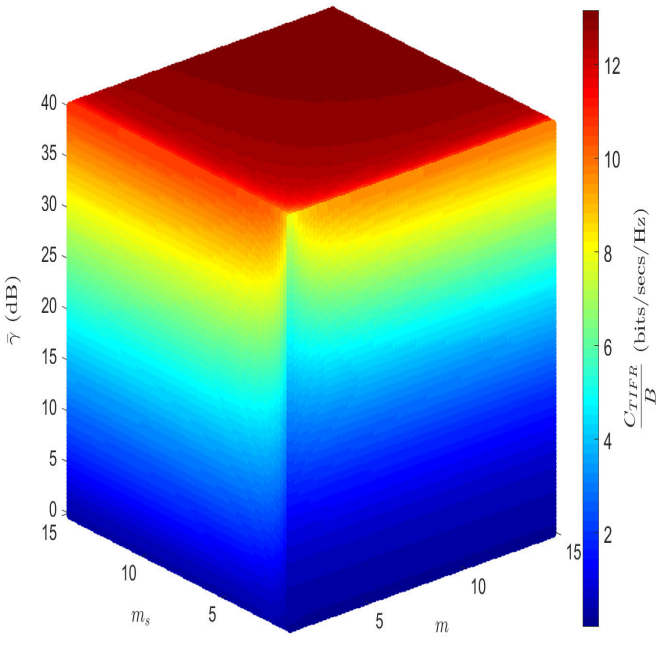


Fig. 2: $C_{\text{TIFR}}/\text{B}$ in an $\mathcal{F}$ fading channel as a function of the $m$, $m_s$ and $\overline{\gamma}$ parameters for $\gamma_0 = 5$ dB.

5 dB. As expected, for both $C_{\text{CIFR}}$ and $C_{\text{TIFR}}$ cases, better performance is achieved at higher $m$, $m_s$ and $\overline{\gamma}$ whereas poor performance is observed at lower $m$, $m_s$ and $\overline{\gamma}$. The difference in the achievable capacity levels is significant since variations of even greater than $30\%$ are noticed between intense and light composite fading conditions across all average SNR regimes. Likewise, Fig. 3 shows the dependence of $C_{\text{TIFR}}/B$ on the cutoff SNR, $\gamma_0$, for two different fading conditions, i.e., intense and moderate composite fading conditions, and five different average SNR values, namely $\overline{\gamma} = \{0, 10, 20, 30, 40\}$ dB. Furthermore, it is observed that when $\gamma_0 = \gamma_{\text{th}}$, the cutoff SNR that maximizes the spectral efficiency ($\gamma_0^*$) increases as $\overline{\gamma}$ increases. When comparing Fig. 3(a) and Fig. 3(b), for fixed $\overline{\gamma}$, the value of $\gamma_0^*$ for the moderate composite fading conditions was greater than that for the intense composite fading conditions. Additionally, for $\gamma_0 < \gamma_0^*$, the curves in Fig. 3(b) are relatively flat compared to that for Fig. 3(a). This verifies that the spectral efficiency improvement provided by truncated channel inversion ($\gamma_0 = \gamma_0^*$), compared to total channel inversion ($\gamma_0 = 0$), is more significant when the channel is subject to severe multipath fading and simultaneous heavy shadowing i.e., intense composite fading conditions.

## V. Conclusion

In this paper, we presented a comprehensive capacity analysis over $\mathcal{F}$ composite fading channels assuming channel inversion with fixed rate. In particular, the tractability of the $\mathcal{F}$ composite fading model led to the determination of the channel

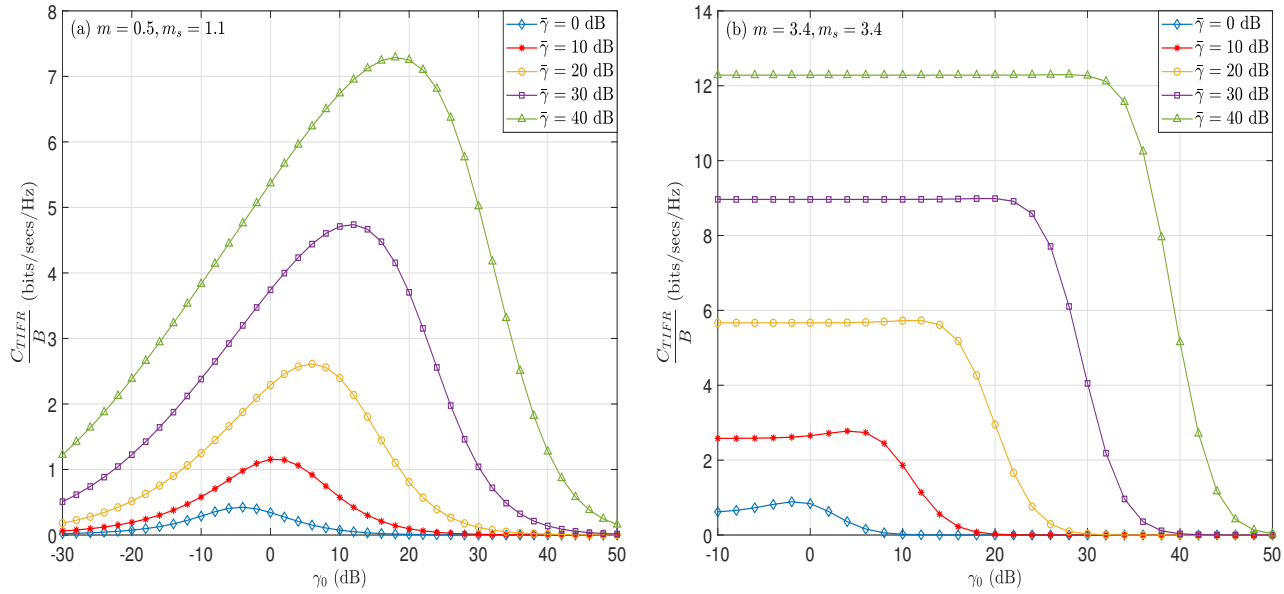


Fig. 3: $C_{\mathrm{TIFR}}/\mathrm{B}$ in an $\mathcal{F}$ fading channel as a function of the $\gamma_0$ for different $\overline{\gamma}$ values for (a) intense and (b) moderate composite fading conditions.

capacity for two distinct cases: i) channel inversion with fixed rate; ii) truncated channel inversion with fixed rate. When comparing these expressions with those for the generalized-$K$ fading channels given in [30], the $\mathcal{F}$ fading model exhibits lower complexity and provides more insights on the impact of the involved parameters on the overall system performance. Based on this, it was shown that the corresponding channel capacity changes considerably even at slight variations of the average SNR and the severity of the multipath fading and shadowing conditions. The impact of different types of $\mathcal{F}$ composite fading was also investigated through comparisons with the respective capacity for the case of a Rayleigh fading channel. This has highlighted that different types of composite fading can have a profound effect which is beyond the range of the fading conditions experienced in a conventional Rayleigh fading environment. Therefore, it is verified that is of paramount importance to ensure accurate characterization of composite fading conditions in future communication systems in order to meet increased quality of service demands associated with stringent power consumption and complexity requirements. Finally, the new results and insights provided here will be useful in the design and deployment of future communications systems. For example when assessing technologies such as channel selection and spectrum aggregation for use in heterogeneous networks, telemedicine and vehicular communications, to name but a few.

## Acknowledgment

This work was supported in part by Khalifa University under Grant No. KU/RC1-C2PS-T2/8474000137 and Grant No. KU/FSU-8474000122, and by the U.K. Engineering and Physical Sciences Research Council under Grant No. EP/L026074/1, by the Department for the Economy Northern Ireland through Grant No. USI080.

## References

[1] H. B. Janes, and P. I. Wells, "Some tropospheric scatter propagation measurements near the radio horizon," *Proc. IRE*, vol. 43, no. 10, pp. 1336–1340, Oct. 1955.

[2] S. Basu et al, "250 MHz/GHz scintillation parameters in the equatorial, polar, and auroral environments," *IEEE J. Sel. Areas Commun.*, vol. 5, no. 2, pp. 102–115, Feb. 1987.

[3] S. O. Rice, "Statistical properties of a sine wave plus random noise," *Bell Labs Tech. J.*, vol. 27, no. 1, pp. 109–157, Jan. 1948.

[4] R. J. C. Bultitude, S. A. Mahmoud, and W. A. Sullivan, "A comparison of indoor radio propagation characteristics at 910 MHz and 1.75 GHz," *IEEE J. Sel. Areas Commun.*, vol. 7, no. 1, pp. 20–30, Jan. 1989.

[5] A. J. Goldsmith, and P. P. Varaiya, "Capacity of fading channels with channel side information," *IEEE Trans. Inf. Theory*, vol. 43, no. 6, pp. 1986–1992, Nov. 1997.

[6] M.-S. Alouini, and A. J. Goldsmith, "Capacity of Rayleigh fading channels under different adaptive transmission and diversity-combining techniques," *IEEE Trans. Veh. Technol.*, vol. 48, no. 4, pp. 1165–1181, Jul. 1999.

[7] ——, "Adaptive modulation over Nakagami fading channels," *Wireless Pers. Commun.*, vol. 13, no. 1-2, pp. 119–143, May 2000.

[8] Q. Zhang, and D. Liu, "A simple capacity formula for correlated diversity Rician fading channels," *IEEE Commun. Lett.*, vol. 6, no. 11, pp. 481–483, Nov. 2002.

[9] D. B. da Costa, and M. D. Yacoub, "Average channel capacity for generalized fading scenarios," *IEEE Commun. Lett.,* vol. 11, no. 12, pp. 949−951, Dec. 2007.

[10] D. B. da Costa, and M. D. Yacoub, "Channel capacity for single branch receivers operating in generalized fading scenarios," *4th International Symposium on Wireless Communication Systems*, 2007, pp. 215−218.

[11] P. S. Bithas, and P. T. Mathiopoulos, "Capacity of correlated generalized gamma fading with dual-branch selection diversity," *IEEE Trans. Veh. Technol.*, vol. 58, no. 9, pp. 5258−5663, Sep. 2009.

[12] P. S. Bithas, G. P. Efthymoglou, and N.C. Sagias, "Spectral efficiency of adaptive transmission and selection diversity on generalised fading channels," *IET Commun.*, vol. 4, no. 17, pp. 2058−2064, Sep. 2010.

[13] M. Matthaiou, N. D. Chatzidiamantis, and G. K. Karagiannidis, "A new lower bound on the ergodic capacity of distributed MIMO systems," *IEEE Signal Process. Lett.*, vol. 18. no. 4, pp. 227−230, Apr. 2011.

[14] J. Zhang, Z. Tan, H. Wang, Q. Huang, and L. Hanzo, "The effective throughput of MISO systems over $\kappa-\mu$ fading channels," *IEEE Trans. Veh. Technol.*, vol. 63, no. 2, pp. 943−947, Feb. 2014.

[15] H. Hashemi, "The indoor radio propagation channel," *Proc. IEEE*, vol. 81, no. 7, pp. 943–968, Jul. 1993.

[16] J. R. Clark, and S. Karp, "Approximations for lognormally fading optical signals," *Proc. IEEE*, vol. 58, no. 12, pp. 1964–1965, Dec. 1970.

[17] A. Abdi, and M. Kaveh, "On the utility of gamma PDF in modeling shadow fading (slow fading)," in *Proc. IEEE VTC*, vol. 3, May 1999, pp. 2308–2312.

[18] A. H. Marcus, "Power sum distributions: An easier approach using the wald distribution," *J. Am. Stat. Assoc.*, vol. 71, no. 353, pp. 237–238, 1976.

[19] H. G. Sandalidis, N. D. Chatzidiamantis, and G. K. Karagiannidis, "A tractable model for turbulence and misalignment-induced fading in optical wireless systems," *IEEE Commun. Lett.,* vol. 20, no. 9, pp. 1904−1907, Sep. 2016.

[20] I. Trigui, A. Laourine, S. Affes, and A. Stéphenne, "The inverse Gaussian distribution in wireless channels: Second-order statistics and channel capacity," *IEEE Trans. Commun.*, vol. 60, no. 11, pp. 3167–3173, Nov. 2012.

[21] A. Abdi, and M. Kaveh, "$K$ distribution: An appropriate substitute for Rayleigh-lognormal distribution in fading-shadowing wireless channels," *IET Electron. Lett.*, vol. 34, no. 9, pp. 851–852, Apr. 1998.

[22] A. Abdi, W. C. Lau, M.-S. Alouini, and M. Kaveh, "A new simple model for land mobile satellite channels: First-and second-order statistics," *IEEE Trans. Wireless Commun.*, vol. 2, no. 3, pp. 519–528, May 2003.

[23] H. Suzuki, "A statistical model for urban radio propagation," *IEEE Trans. Commun.*, vol. 25, no. 7, pp. 673–680, Jul. 1977.

[24] G. E. Corazza, and F. Vatalaro, "A statistical model for land mobile satellite channels and its application to nongeostationary orbit systems," *IEEE Trans. Veh. Technol.*, vol. 43, no. 3, pp. 738–742, Aug. 1994.

[25] I. M. Kostić, "Analytical approach to performance analysis for channel subject to shadowing and fading," *IEE Proc. Comm.*, vol. 152, no. 6, pp. 821–827, Dec. 2005.

[26] R. Agrawal, "On the efficacy of Rayleigh-inverse Gaussian distribution over $K$-distribution for wireless fading channels," *Wireless Commun. Mob. Comput.*, vol. 7, no. 1, pp. 1–7, Jan. 2007.

[27] P. S. Bithas, "Weibull-gamma composite distribution: alternative multipath/shadowing fading model," *IET Electronics Letters*, vol. 45, no. 14, pp. 749−751, Jul. 2009.

[28] P. C. Sofotasios, T. A. Tsiftsis, M. Ghogho, L. R. Wilhelmsson, and M. Valkama, "The $\eta$-$\mu$ / $IG$ distribution: A novel physical multipath/shadowing fading model," in *Proc. IEEE International conference on Communications (IEEE ICC '13)*, Jun. 2013, pp. 5715–5719.

[29] A. Abdi, and M. Kaveh, "Comparison of DPSK and MSK bit error rates for $K$ and Rayleigh-lognormal fading distributions," *IEEE Commun. Lett.*, vol. 4, no. 4, pp. 122–124, Apr. 2000.

[30] A. Laourine, M.-S. Alouini, S. Affes, and A. Stephenne, "On the capacity of generalized-$K$ fading channels," *IEEE Trans. Wireless Commun.*, vol. 7, no. 7, pp. 2441–2445, Jul. 2008.

[31] F. Yilmaz, and M.-S. Alouini, "A new simple model for composite fading channels: Second order statistics and channel capacity," in *Proc. ISWC*, Sep. 2010, pp. 676–680.

[32] P. S. Bithas, N. C. Sagias, P. T. Mathiopoulos, G. K. Karagiannidis, and A. A. Rontogiannis, "On the performance analysis of digital communications over generalized-$K$ fading channels," *IEEE Commun. Lett.*, vol. 10, no. 5, pp. 353–355, May 2006.

[33] L. Moreno-Pozas, F. J. Lopez-Martnez, J. F. Paris and E. Martos-Naya, "The $\kappa-\mu$ shadowed fading model: Unifying the $\kappa-\mu$ and $\eta-\mu$ distributions," *IEEE Trans. Veh. Technol.*, vol. 65, no. 12, pp. 9630−9641, Dec. 2016.

[34] J. F. Paris, "Statistical characterization of $\kappa-\mu$ shadowed fading," *IEEE Trans. Veh. Technol.*, vol. 63, no. 2, pp. 518−526, Feb. 2014.

[35] M. C. Clemente, and J. F. Paris, "Closed-form statistics for sum of squared Rician shadowed variates and its application, *IET Electr. Lett.*, vol. 50, no. 2, pp. 120−121, Jan. 2014.

[36] P. S. Bithas, N. C. Sagias, P. T. Mathiopoulos, S. A. Kotsopoulos, A. M. Maras, "On the correlated $K$ - distribution with arbitrary fading parameters," *IEEE Signal Proc. Lett.*, vol. 15, no. 7, pp. 541−544, Jul. 2008.

[37] J. Zhang, M. Matthaiou, Z. Tan, and H. Wang, "Performance analysis of digital communication systems over composite $\eta-\mu$/gamma fading channels," *IEEE Trans. Veh. Technol.*, vol. 61, no. 7, pp. 3114−3124, Jul. 2012.

[38] N. D. Chatzidiamantis, and G. K. Karagiannidis, "On the distribution of the sum of gamma-gamma variates and applications in RF and optical wireless communications," *IEEE Trans. Commun.*, vol. 59, no. 5, pp. 1298−1308, May 2011.

[39] M. Matthaiou, N. D. Chatzidiamantis, G. K. Karagiannidis, and J. A. Nossek, "On the capacity of generalized − fading MIMO channels," *IEEE Trans. Signal Proc.*, vol. 58, no. 11, pp. 5939−5944, Nov. 2010.

[40] M. Matthaiou, N. D. Chatzidiamantis, G. K. Karagiannidis, and J. A. Nossek, "ZF detectors over correlated $K$ fading MIMO channels," *IEEE Trans. Commun.*, vol. 59, no. 6, pp. 1591−1603, June 2011.

[41] C. Zhong, M. Matthaiou, G. K. Karagiannidis, A. Huang, and Z. Zhang, "Capacity Bounds for AF Dual-hop Relaying in Fading Channels," *IEEE Trans. Veh. Technol.*, vol. 61, no. 4, pp. 1730−1740, Apr. 2012.

[42] X. Li, J. Li, L. Li, J. Jin, J. Zhang, and Di Zhangm, "Effective rate of MISO systems over $\kappa-\mu$ shadowed fading channels," *IEEE Access*, vol. 5, no. 3, pp. 10605−10611, Apr. 2017.

[43] M. You, H. Sun, J. Jiang, and J. Zhang, "Unified framework for the effective rate analysis of wireless communication systems over MISO fading channels," *IEEE Trans. Commun.*, vol. 65, no. 4, pp. 1775−1785 Apr. 2017.

[44] J. Zhang, L. Dai, W. H. Gerstacker, and Z. Wang, "Effective capacity of communication systems over $\kappa-\mu$ shadowed fading channels," *IET Electronics Letters*, vol. 51, no. 19, pp. 1540−1542, Oct. 2015.

[45] K. P. Peppas, P. T. Mathiopoulos, and J. Yang, "On the effective capacity of amplify-and-forward multihop transmission over arbitrary and correlated fading channels," *IEEE Wireless Commun.*, vol. 5, no. 3, pp. 248−251, Mar. 2016.

[46] A. Laourine, M.-S. Alouini, S. Affes, and A. Stéphenne, "On the performance analysis of composite multipath/shadowing channels using the $\mathcal{G}$-distribution," *IEEE Trans. Commun.*, vol. 57, no. 4, pp. 5715−5719, Apr. 2009.

[47] F.S. Almehmadi, and O.S. Badarneh, "On the effective capacity of Fisher−Snedecor F fading channels," *IET Electronics Letters*, vol. 54, no. 18, pp. 1068−1070, Oct. 2018.

[48] S. Chen, J. Zhang, G. K. Karagiannidis, and Bo Ai, "Effective rate of MISO systems over Fisher-Snedecor F fading channels" *IEEE Commun. Lett.*, Accepted

[49] S. K. Yoo, S. Cotton, P. Sofotasios, M. Matthaiou, M. Valkama, and G. Karagiannidis, "The Fisher-Snedecor $\mathcal{F}$ distribution: A simple and accurate composite fading model," *IEEE Commun. Lett.*, vol. 21, no. 7, pp. 1661–1664, Jul. 2017.

[50] M. Nakagami, *The $m$-distribution − A general formula of intensity distribution of rapid fading*. Elsevier, 1960.

[51] I. S. Gradshteyn and I. M. Ryzhik, *Table of Integrals, Series, and Products*, 7th ed. London: Academic Press, 2007.

[52] M. K. Simon, and M.-S. Alouni, *Digital Communication over Fading Channels*, 2nd ed. New York: Wiley, 2005.

[53] A. P. Prudnikov, Yu. A. Brychkov, and O. I. Marichev, *Integrals and Series*, 3rd ed. New York: Gordon and Breach Science, vol. 1, Elementary Functions, 1992.

[54] F. Yilmaz, and M.-S. Alouini, "Novel asymptotic results on the high-order statistics of the channel capacity over generalized fading channels," *in Proc. of IEEE International Workshop on Signal Processing Advances in Wireless Communications (SPAWC 2012)*, Cesme, Turkey, Jun. 2012, pp. 389–393.

[55] I. S. Ansari, M.-S. Alouini, and J. Cheng, "On the Capacity of FSO Links under lognormal and Rician-lognormal turbulences," *IEEE Vehicular Technology Conference Fall 2014 (VTC '14 Fall)*, Vancouver, Canada, Sep. 2014, pp. 1–6.

[56] Z. Ji, C. Dong, Y. Wang, and J. Lu "On the analysis of effective capacity over generalized fading channels," *IEEE International Conference on Communications (ICC '14)*, Sydney, Australia, June 2014, pp. 1977–1983.

[57] J. Zhang, L. Dai, Z. Wang, D. Wing Kwan Ng, and W. H. Gerstacker, "Effective rate analysis of MISO systems over $\alpha-\mu$ fading channels," *IEEE Global Conference on Communications (Globecom '15)*, San Diego, USA, Dec. 2015, pp. 1–6.

[58] M. You, H. Sun, J. Jian, and J. Zhang, "Unified framework for the effective rate analysis of wireless communication systems over MISO fading channels," *IEEE Trans. Commun.*, vol. 65, no. 4, pp. 1775–1785, Apr. 2017.